Noncontact common-path Fourier domain optical coherence tomography method for *in vitro* intraocular lens power measurement

Yong Huang
Kang Zhang
Jin U. Kang
Don Calogero
Robert H. James
Ilko K. Ilev

Noncontact common-path Fourier domain optical coherence tomography method for *in vitro* intraocular lens power measurement

Yong Huang,[a,b] **Kang Zhang,**[c] **Jin U. Kang,**[b] **Don Calogero,**[a] **Robert H. James,**[a] **and Ilko K. Ilev**[a]
[a]U.S. Food and Drug Administration, Center for Devices and Radiological Health, 10903 New Hampshire Avenue, Silver Spring, Maryland 20993
[b]Johns Hopkins University, Department of Electrical and Computer Engineering, 3400 N. Charles Street, Baltimore, Maryland 21218
[c]GE Global Research, 1 Research Circle, Niskayuna, New York 12309

Abstract. We propose a novel common-path Fourier domain optical coherence tomography (CP-FD-OCT) method for noncontact, accurate, and objective *in vitro* measurement of the dioptric power of intraocular lenses (IOLs) implants. The CP-FD-OCT method principle of operation is based on simple two-dimensional scanning common-path Fourier domain optical coherence tomography. By reconstructing the anterior and posterior IOL surfaces, the radii of the two surfaces, and thus the IOL dioptric power are determined. The CP-FD-OCT design provides high accuracy of IOL surface reconstruction. The axial position detection accuracy is calibrated at 1.22 μm in balanced saline solution used for simulation of *in situ* conditions. The lateral sampling rate is controlled by the step size of linear scanning systems. IOL samples with labeled dioptric power in the low-power (5D), mid-power (20D and 22D), and high-power (36D) ranges under *in situ* conditions are tested. We obtained a mean power of 4.95/20.11/22.09/36.25 D with high levels of repeatability estimated by a standard deviation of 0.10/0.18/0.2/0.58 D and a relative error of 2/0.9/0.9/1.6%, based on five measurements for each IOL respectively. The new CP-FD-OCT method provides an independent source of IOL power measurement data as well as information for evaluating other optical properties of IOLs such as refractive index, central thickness, and aberrations. © *2011 Society of Photo-Optical Instrumentation Engineers (SPIE).* [DOI: 10.1117/1.3660313]

Keywords: cataract; intraocular lens dioptric power; common-path Fourier domain optical coherence tomography.

Paper 11257RR received May 23, 2011; revised manuscript received Sep. 27, 2011; accepted for publication Oct. 24, 2011; published online Nov. 23, 2011.

1 Introduction

Intraocular lens (IOL) implantation in refractive cataract surgery has become one of the most commonly performed surgical operations in medicine with more than 500 million IOLs implanted worldwide since the invention and first implantation of IOLs in 1949.[1] Cataracts affect more than 20 million Americans over the age of 40 and every year more than 3 million cataract surgeries are performed.[2] These numbers will dramatically increase over the next 20 years as the U.S. population ages.[2] Most of the cataract post-surgical device-associated complications are directly related to some fundamental IOL optical properties such as dioptric power, reflected glare, light scattering, imaging quality, material refractive-index, thickness, and geometrical shape. The focal length (or IOL dioptric power) is a key parameter whose precise preclinical measurement is part of release specifications for all IOLs and is of critical importance to the safety and effectiveness of IOLs.[3,4] Currently, some conventional techniques for IOL dioptric power measurements are utilized, such as image magnification, autocollimation, nodal slide, Bessel's method, Moiré deflectometry, Talbot interferometry, and confocal fiber-optic laser microscopy.[3–10] The effectiveness of most of these methods is often limited in terms of accuracy, spatial sampling alignments, subjective image evaluation, and the dynamic range over which measurements can be performed (for both positive and negative dioptric powers). Moreover, three standard test methods for measurement of IOL dioptric power are specified by the International Standard, ISO 11979-2:1999 Ophthalmic Implants-Intraocular Lenses, Part 2: Optical properties and test methods.[11] One of these standard methods is for determination of dioptric power by calculation from measured IOL dimensions including the sample surface radii and central thickness. For measurement of these basic IOL parameters, a specialized radius meter, micrometer, or general purpose interferometer are recommended. These techniques, however, impose some limitations related to requirements for either a sensor-to-surface mechanical contact or complex and nonpractical measurements for *in situ* condition usage. In addition, the small size of IOLs also makes the measurement of surface radii highly demanding. Because of the complexity in correcting the IOL dimensions obtained under non-*in situ* conditions, alternative noncontact methods that could be performed in a wet environment (IOL in balanced saline solution) are of great interest.

Optical coherence tomography is now established as a powerful and versatile tool for *in vivo* optical biopsy.[12] It has been used to perform *in vivo* quantitative corneal parameter extraction including anterior and posterior radii of curvature, central corneal optical power, and thickness maps of the cornea.[13]

Address all correspondence to: Yong Huang, The Johns Hopkins University, Department of Electrical and Computer Engineering, 3400 North Charles Street, Barton Hall 402, Baltimore, Maryland 21218; Tel: 410-900-5453; Fax: 410-516-5566; E-mail: yhuang60@jhu.edu.
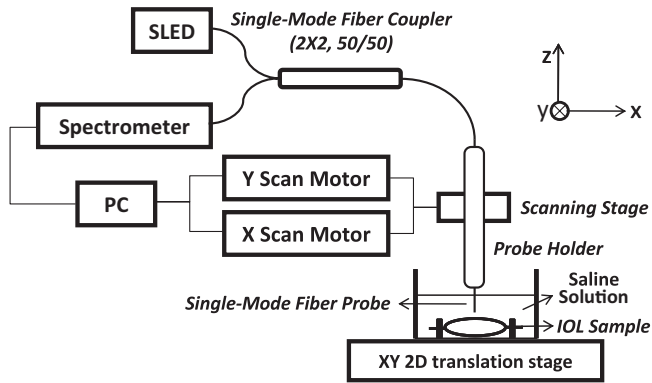
Fig. 1 Schematic of the system setup.

Fig. 2 Comparison of 1D sample arm beam geometry of CP-OCT and standard Galvo scanner based OCT. (a) Illustration of fan distortion in standard Galvo scanner based OCT; (b) illustration of distortion caused by the refraction at the air-solution interface; (c) illustration of CP-OCT scanning beam geometry. (Dashed line: trajectory of scanning beam; L1: focal lens; OPL: optical path length; Δz: projection of OPL on the z-axis.)

However, due to the scanner nontelecentricity or fan distortion[14] of the scanning beam and the refraction at the corneal surface, algorithms for all those corrections were required to extract the correct parameters.[13–16] By sharing reference and probe arm, the common-path Fourier domain optical coherence tomography (CP-FD-OCT) is a straightforward and effective technique that circumvents group velocity dispersion and polarization compensation to maintain a high axial resolution with a simple principal setup.[17,18] In this work, in order to avoid the fan distortion of the scanning beam, we have performed the scanning procedures using step motors. Furthermore, the fiber probe is immersed into the saline solution, thus the refraction of the light at the solution-air interface is avoided. Although there is limited adjustment on the reference arm light power to optimize the signal-to-noise ratio (SNR),[19] such a deviation from the optimized SNR is acceptable considering the advantages of CP-OCT. In this paper we demonstrate, for the first time to the best of our knowledge, a novel and simple CP-FD-OCT method for noncontact, accurate, and objective measurement of IOL dioptric powers under *in situ* conditions which could provide valuable information for standards, regulation, and development.

2 Methods

The CP-FD-OCT method principal setup is illustrated in Fig. 1. The IOL dioptric power measurement method is based on a digital IOL surface reconstruction by scanning a single-mode fiber probe along x and y directions utilizing two high-resolution linear motors. The IOL sample is fitted into a customized lens holder in a glass cuvette filled with balanced saline solution. The light from a Superlum Broadband Light Source (825.1-nm center wavelength, 67-nm bandwidth, 10 mW) is coupled into a single-mode fiber by a 50/50 broadband coupler. The single-mode fiber probe is cleaved at a right angle to provide Fresnel reflection at the fiber end which serves as the reference light. The power of the beam illuminating the sample was measured to be 630 μW. The single-mode fiber is placed into a fiber holder attached to a Newport *XYZ* three-dimensional (3D) translation stage driven by high-resolution linear stepper motors (Newport 850G, 1 μm resolution). The back reflected/scattered light from the reference and the sample is directly coupled into the fiber probe and routed by the coupler to a spectrometer (HR 4000, Ocean Optics) with 3648 pixel line-scan CCD detector, the exposure time is set at 6 ms to get a reasonable reference signal.

Note that the relative smaller refractive index difference of the saline solution and the single-mode fiber requires longer exposure time than air-fiber interface. The CP-OCT system has a theoretical imaging depth of 2.2 mm in saline solution.

The CP-OCT method provides the advanced feature of distortion-free in the sample arm beam geometry. The distortion effects are mainly caused by two sources: fan distortion of the scanning beam and light refraction in the air-saline solution interface. Figure 2(a) illustrates a one-dimensional (1D) fan distortion; note that fan distortion occurs two dimensionally. The fan distortion will cause a flat surface to appear curved in the obtained image. When the light in the sample arm arrives at the air-saline interface with an incident angle other than zero, refraction will occur. As shown in Fig. 2(b), the actual optical path length (OPL) obtained, which the OCT system measures, is not the exact projection distance on the z-axis. Some specialized fan distortion and 3D refraction correction algorithms need to be applied to extract the correct curvature information of the sample. However, the CP-OCT approach is straightforward without fan distortion and refraction as shown in Fig. 2(c). The scanning surface of the fiber tip is a flat surface which is adjusted parallel to the plane of translation stage where the IOL sample lies. Furthermore, the fiber probe is immersed into the saline solution, and thus there is no refraction effect that occurred at the air-saline interface. The fiber probe measures the exact distance along the z-axis from the probe tip to the IOL surface. The fiber tip is positioned as close as possible to the IOL surface in order to get a high SNR during the measurement.

After taking a fast Fourier transform (FFT) of the interpolated spectrum data in linear k-space at each scanning point, the distance between the reference (fiber probe tip) and IOL sample surface can be resolved with an accuracy of 1.22 μm by searching where the maximum peak signal of the A-scan data lies.[20–22] The accuracy is determined by the OCT system and refractive index of saline solution at wavelength around 825.1 nm. The peak position detection accuracy can be further improved by using the zero padding technique to spectral data before FFT.[19]
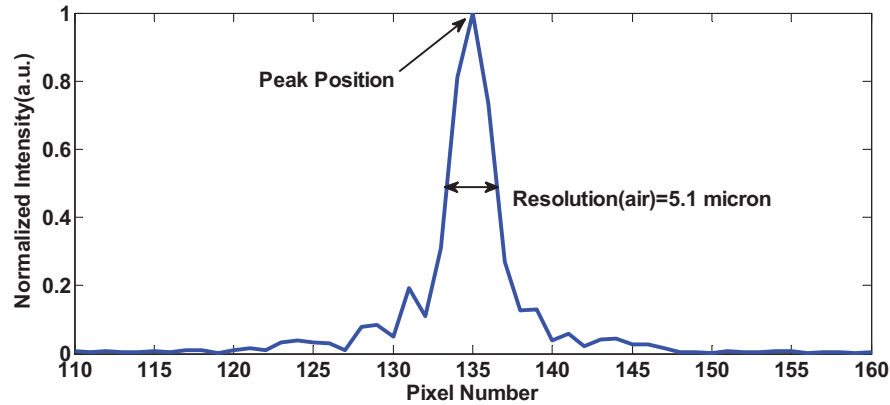
Fig. 3 Illustration for peak-position and system resolution.

The peak position and system axial resolution is illustrated in Fig. 3. In this case, accuracy higher than the axial resolution (5.1 μm in air/3.9 μm in saline solution) of the OCT system can be achieved because there is only one boundary between the saline solution and the IOL sample. The maximum signal intensity comes from this boundary in the A-scan distance profile. By searching for the maximum signal intensity, we can determine where the surface lies. Thus, we can locate the peak signal position with a resolution of one pixel which corresponds to 1.6 μm in air and 1.22 μm in saline solution. These were calibrated by measuring the displacement of an ideal mirror surface immersed in saline solution controlled by a high-precision micrometer using the OCT system, as geometrical distance needs to be corrected by the refractive index of the saline solution at the OCT system wavelength band.

The lateral scan is carried out with a field of view centered on the highest point of the IOL sample surface. The size of the field of view for 5D is 3×3 mm (150×150 points, step size is 20 μm), for 20D and 22D it is 3×3 mm (100×100 points, step size is 30 μm) and for 36D it is 1.5×1.5 mm (150×150, step size is 10 μm). The total acquisition time is proportional to the total sampling points. For a 150×150 scanning protocol, the acquisition time is about 2.5 h. The acquisition time can be significantly reduced by modifying the scanning program, which is in progress now. Later, the radii of two IOL surfaces can be calculated after a digital construction. The OCT signal intensity decays when the distance between the surface and the fiber tip increases, as the beam coming out of the fiber probe

is divergent. A 20 dB decay of the OCT signal intensity from depth 100 to 500 μm was observed by using a mirror as the sample. The CP-OCT system has a sensitivity range of around 70 dB over a distance of 2 mm. The glass cuvette is placed on an *XY* two-dimensional translation stage. By adjusting the sample position and the height of the scanning stage, the probe can be positioned pointing to the center of the IOL sample. Then the sample stage is moved back a distance of half of the length of field of view along the *x* and *y* directions, and the scan is initiated. Following the completion of the first IOL surface scan, the IOL is flipped over and identical procedures for the second surface are repeated.

Due to the limit of identifying two surfaces of the IOL during a single scan in wet condition, the thickness of the IOL is measured in air. For the thickness measurement, one B-scan image is shown in Fig. 4, which is cropped to show the area of interest. It is in log scale along the axial direction to accommodate details far away from the probe. The physical central thickness of the IOL sample t_c can be resolved by two horizontal black lines marked in the image. The bottom black line indicates the surface on which the IOL sample rests.[23] Artifacts below the bottom line are ghost images due to the multiple reflections. A typical *in vitro* B-mode image of the IOL sample in wet condition is shown in Fig. 5 in linear scale, which is also cropped to show the area of interest.

The key CP-FD-OCT method idea involves the specific use of motor driving scanning common-path Fourier domain optical coherence tomography, which has the following advantages:
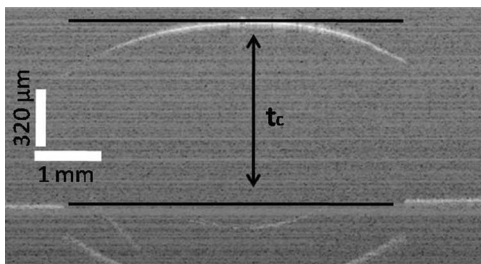
Fig. 4 B-scan image in air with the lens resting on a flat plate, that the upper arc is the anterior surface of the lens and that the rear surface is located by the plane of the back plate. (Two horizontal black lines indicate the thickness of IOL, t_c.)
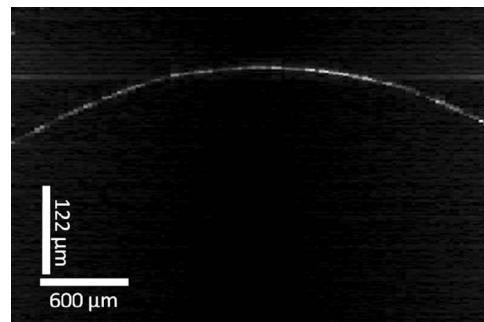
Fig. 5 A typical *in vitro* B-mode image of the IOL sample consists of 100 A-scans.

1. The scanning beam field forms a flat plane when the fiber tip is driven two dimensionally. This flat plane guarantees that the curvature calculated from the measurement is accurate. An alternative procedure uses the mirror scanning setup, which is another commonly used method to perform beam scanning in FD-OCT. However, in this case, the scanning beam field has intrinsic curvature. Hence, we chose the motor driven scanning to remove curvature error. 2. By creating a reference from the single-mode fiber tip, the group velocity dispersion and polarization mismatch between the reference and sample arms are circumvented in real time. Dispersion and polarization mismatch is caused by the sample and saline solution only. However, the mismatch over a distance of 1-mm thick saline solution is negligible. 3. It is a completely noncontact method, and therefore has no effect on the IOL sample. 4. It is an *in situ* measurement method. Due to the small size of the single-mode fiber probe, which has a diameter of 50 μm after removing the cladding and the mechanical hardness of the probe, it can be inserted into the saline solution for a long time while maintaining the shape and reference easily. 5. Measurement environmental conditions can be easily maintained at a stable stage due to the small size of the fiber probe inserted into the solution and the slow motor driving speed, 0.1 mm/s, used in the experiment. 6. Surface reconstruction can provide valuable information to improve standards and regulations, since the radii of front and back surfaces are calculated separately.

For further data analysis, we utilize the following procedures. First, we construct the measurement surface using a peak detection method for each A-scan shown in Figs. 6(a) and 6(b). Second, we perform a third degree polynomial surface fitting using the toolbox in MATLAB 2010b. Points that deviate over 10 μm from the fitting surface are excluded from the fitting data to improve the accuracy of fitting, shown in Fig. 6(c) (top). Residuals of the fitting and experimental data are presented in Fig. 6(c) (bottom). Third, the lowest point (x_0, y_0) of the surface is calculated based on the polynomial fitting equation. Using parameters up to the second order of the equation and the condition for a minimum value, the start point (x_{start}, y_{start}) can be calculated. Then, the lowest point (x_0, y_0) is searched around the start point. Fourth, according to geometric mathematics, the surface mean radius can be calculated at the point (x_0, y_0) using the geometric mean of radius along two directions shown in Fig. 6(d), since the IOL is not perfectly spherically symmetric. Finally, with both of the radii and index known, the dioptric power can be determined using the following formula:[11]

$$D = D_f + D_b - (t_c/n_{\mathrm{IOL}})D_f D_b \qquad (1)$$

where D is the dioptric power,

$$D_f = (n_{\mathrm{IOL}} - n_{\mathrm{med}})/r_f, \qquad (2)$$

$$D_b = (n_{\mathrm{med}} - n_{\mathrm{IOL}})/r_b, \qquad (3)$$

n_{IOL} is the refractive index of the IOL optical material (1.459) which is normally provided by the manufacturer, n_{med} is the refractive index of the surrounding medium (1.335), r_f and r_b are the radii of the front and back surface of the lens, respectively, and t_c is the central thickness of the IOL.

3 Results and Discussion

The IOL dioptric power is now determined in compliance with the International Standard, ISO 11979-2:1999 Ophthalmic Implants-Intraocular Lenses, Part 2: Optical properties and test methods.[11] Basic requirements for the measurement methods are listed in the standard including the allowed tolerances on IOL dioptric power: ± 0.3D for the dioptric power range of 0 to $\leq$15D; ± 0.4D for $>$15 to $\leq$ 25D; ± 0.5D for $>$25 to $\leq$30D; and ± 1.0 D for $>$30D.

Using the proposed measurement system and procedures described above, we tested four IOL samples with positive dioptric power of 5D, 20D, 22D, and 36D, which are among in practice low-, middle-, and high-range IOLs that are commonly used. The measured average values of these four lenses are 4.95/20.11/22.09/36.25 D, respectively, based on five measurements. The repeatability is estimated by the standard deviation (SD) of these five measurements, which is 0.1/0.18/0.2/0.58 D for 5/20/22/36 D IOLs, corresponding to a relative error of 2/0.9/0.9/1.6% for four lenses, respectively. Although the SD is relatively larger compared to 0.03D[3]/0.15D[10] obtained by using other conventional test methods, the SD of the new method is well within the allowed tolerances of the ISO Standard. Moreover, as a noncontact and *in situ* compatible approach, the new method can provide additional unique information about the IOL sample, such as the front and back surface radii separately and the central thickness, which turns out to be of great interest to improving the product efficacy and safety. Furthermore, a significant advantage of this method is the absence of evident limitations in using it to test various IOL samples in terms of dioptric power range, negative/positive powers, hydrophilic/hydrophobic, and recently developed new IOL designs. In addition, some other IOL optical properties may also be calculated from the digital surface reconstruction, such as aberrations, though not a main task of this article.

The CP-FD-OCT method accuracy of IOL dioptric power measurement depends on the following basic factors. 1. OCT system sensitivity: The accuracy of determining the peak position of each A-scan is critical to the digital surface reconstruction. However, sensitivity of the OCT system degrades as the probe moves away from the sample surface.[24] The error increases when the probe goes to the margin of the IOL scan, as the distance between the IOL surface and probe is increasing and the beam coming out of the fiber probe is divergent. It is important to position the IOL surface as close to the fiber tip as possible. 2. Lateral scanning step size: The optical lateral resolution of the CP-OCT system varies over the depth as the beam coming out of the bare fiber probe is divergent. The lateral resolution is measured to be 7.5 μm when the sample is 100 μm away from the fiber tip. It goes up to 22 μm when the distance is 0.5 mm. During the measurement, the distance from the fiber tip to the IOL surface is usually within a 500 μm range. When the step size of the motor is larger than the optical lateral resolution, the system resolution is determined by the step size. When the step size of the motor is smaller than the optical lateral resolution, the IOL surface is oversampled. At each lateral position we can obtain an averaged distance over the field of the optical lateral resolution, which should be the distance from the fiber tip to the center part of the field. During the

(a)

(b)

(c)

(d)
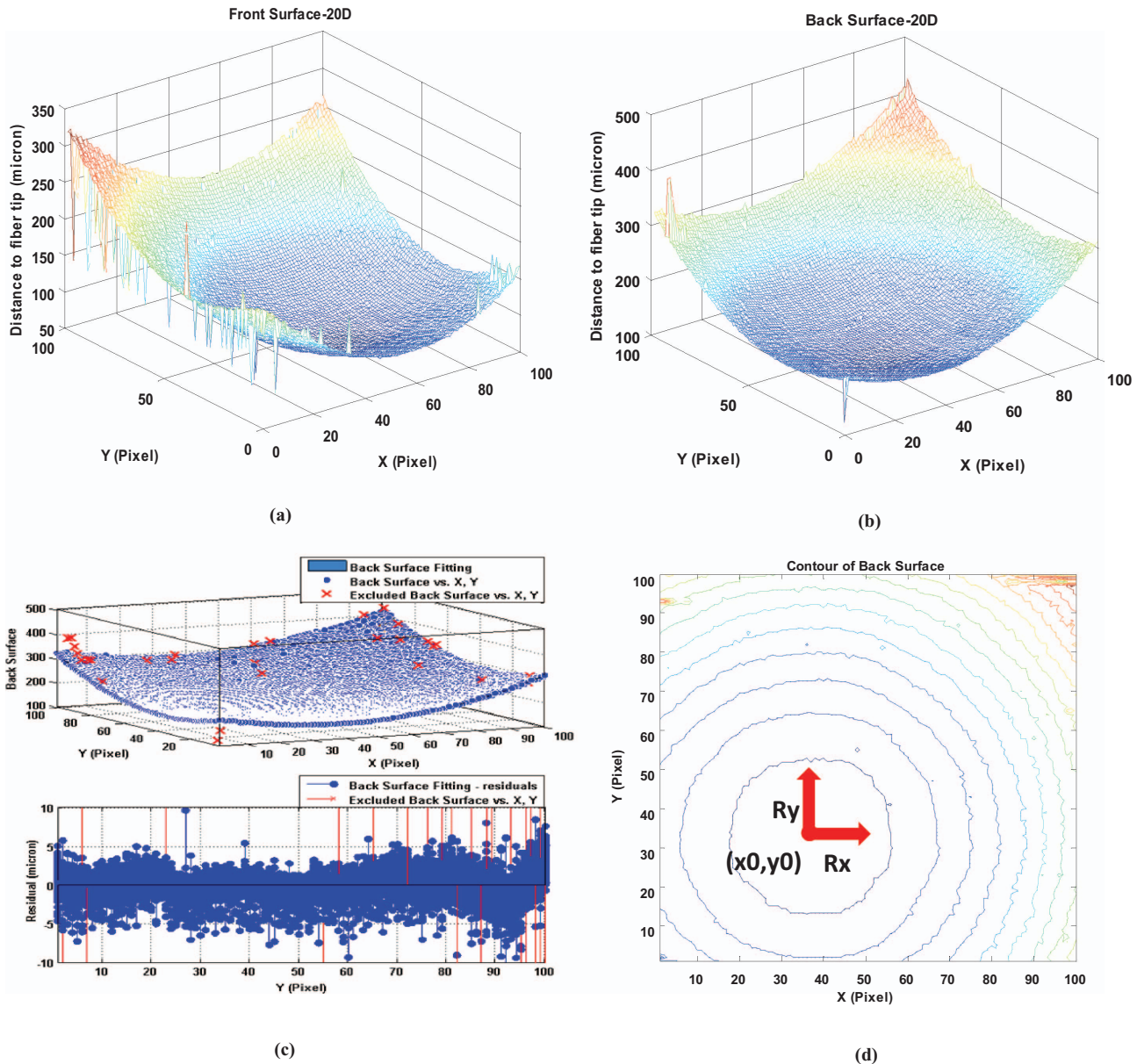
Fig. 6 (a) Front surface of 20D IOL sample constructed by peak position detection of each A-scan; (b) back surface of 20D IOL sample constructed by peak detection of each A-scan (blue to red indicating low to high); (c) top: third degree polynomial surface fitting of the experimental data of back surface; bottom: residuals of the fitting; (d) mean radius of surface is the geometric mean of radius along two directions (*Rx* and *Ry*) shown in a contour image of the back surface.

measurement of IOL, the highly curved surface may prevent some signal within the resolution area being collected back through the fiber. Degradation of the resolution over the depth further decreases the signal intensity. This is the reason for the error to go up when the probe scans the edge area of IOL and for the error increase with the IOL dioptric power increase. In order to cover a large field of view including reasonable total sampling points, different step sizes were used depending on the dioptric power of the IOL samples. By reducing the step size, increasing the number of scanning points, and performing zero-padding to the spectra data before FFT, a digital surface reconstruction with a higher accuracy can be achieved, thus providing more accurate radius calculation.

4 Conclusion

We have demonstrated a novel simple method (CP-FD-OCT) for measuring the dioptric power of various IOLs. It is a noncontact, *in situ* measurement approach that could provide accurate, objective, stable, and cost effective measurement of the dioptric power of various IOL designs. Furthermore, it can provide a new tool for monitoring the quality of IOLs.

The mention of commercial products, their sources, or their use in connection with material reported here is not to be construed as either an actual or implied endorsement of such products by the U.S. Food and Drug Administration (FDA).

References

1. D. Apple and J. Sims, "Harold Ridley and the invention of the intraocular lens," *J. Surv. Ophthalmol.* **40**, 279–292 (1996).
2. National Eye Institute, *Arch. Ophthalmol.* (accessed January 16, 2011), http://www.nei.nih.gov/eyedata/pbd6.asp.
3. I. Ilev, "A simple confocal fibre-optic laser method for intraocular lens power measurement," *Eye* **21**, 819–823 (2007).
4. K. Hoffer, D. Calogero, R. Faaland, and I. Ilev, "Precise testing of the dioptric power accuracy of exact-power-labeled intraocular lenses," *J. Cataract Refractive Surg.* **35**, 1995–1999 (2009).
5. W. J. Smith, *Modern Optical Engineering*, 2nd Ed., McGraw-Hil, New York (1990).
6. Y. Nakano and K. Murata, "Talbot interferometry for measuring the focal length of a lens," *Appl. Opt.* **24**, 3162–3166 (1985).
7. D. Su and C. Chang, "A new technique for measuring the effective focal length of a thick lens or a compound lens," *Opt. Commun.* **78**, 118–122 (1990).
8. E. Keren, K. Kreske, and O. Kafri, "Universal method for determining the focal length of optical systems by moiré deflectometry," *Appl. Opt.* **27**, 1383–1385 (1988).
9. D. Tognetto, G. Sanguinetti, P. Sirotti, P. Cecchini, L. Marcucci, E. Ballone, and G. Ravalico, "Analysis of the optical quality of intraocular lenses," *Invest. Ophthalmol. Visual Sci.* **45**, 2682–2690 (2004).
10. N. E. Norrby, L. Grossman, E. Geraghry, C. Kreiner, M. Mihori, A. Parel, V. Portney, and D. Silberman, "Accuracy in determining intraocular lens dioptric power assessed by interlaboratory tests," *J. Cataract Refractive Surg.* **22**, 983–987 (1996).
11. ISO 11979-2, International Standard, Ophthalmic Implants-Intraocular Lenses-Part 2: Optical Properties and Test Methods (1999).
12. D. Huang, E. Swanson, C. Lin, J. Schuman, W. Stinson, W. Chang, M. Hee, T. Flotte, K. Gregory, C. Puliafito, and J. Fujimoto, "Optical coherence tomography," *Science* **254**, 1178–1181 (1991).
13. M. Zhao, A. Kuo, and J. Izatt, "3D refraction correction and extraction of clinical parameters from spectral domain optical coherence tomography of the cornea," *Opt. Express* **18**, 8923–8936 (2010).
14. S. Ortiz, D. Siedlecki, L. Remon, and S. Marcos, "Optical coherence tomography for quantitative surface topography," *Appl. Opt.* **48**, 6708–6715 (2009).
15. R. Zawadzki, C. Leisser, R. Leitgeb, M. Pircher, and A. Fercher, "Three-dimensional ophthalmic optical coherence tomography with a refraction correction algorithm," *Proc. SPIE* **5140**, 20–27 (2003).
16. S. Ortiz, D. Sledleckl, I. Grulkowski, L. Remon, D. Pascual, M. Wojtkowski, and S. Marcos, "Optical distortion correction in optical coherence tomography for quantitative ocular anterior segment by three-dimensional imaging," *Opt. Express* **18**(3), 2782–2796 (2010).
17. A. Vakhtin, D. Kane, W. Wood, and K. Peterson, "Common-path interferometer for frequency-domain optical coherence tomography," *Appl. Opt.* **42**, 6953–6958 (2003).
18. J. Kang, J.-H. Han, X. Liu, Z. Kang, C. Song, and P. Gehlbach, "Endoscopic functional Fourier domain common path optical coherence tomography for microsurgery," *IEEE J. Sel. Top. Quantum Electron.* **16**, 781–792 (2010).
19. Y. Mao, S. Chang, E. Murdock, and C. Flueraru, "Simultaneous dual—wavelength-band common-path swept-source optical coherence tomography with single polygon mirror scanner," *Opt. Lett.* **36**, 1990–1992 (2011).
20. R. Leitgeb, W. Drexler, A. Unterhuber, B. Hermann, T. Bajraszewski, T. Le, A. Stingl, and A. Fercher, "Ultrahigh resolution Fourier domain optical coherence tomography," *Opt. Express* **12**, 2156–2165 (2004).
21. D. Stifter, A. D. Sanchis Dufau, E. Breuer, K. Wiesauer, P. Burgholzer, O. Hoglinger, E. Gotzinger, M. Pircher, and C. K. Hitzenberger, "Polarization-sensitive optical coherence tomography for material characterisation and testing," *Insight* **47**, 209–212 (2005).
22. M. Shahidi, Z. Wang, and R. Zelkha, "Quantitative thickness measurement of retinal layers imaged by optical coherence tomography," *Am. J. Ophthalmol.* **139**, 1056–1061 (2005).
23. S. Uhlhorn, D. Borja, F. Manns, and J.-M. Parel, "Refractive index measurement of the isolated crystalline lens using optical coherence tomography," *Vision Res.* **48**, 2732–2738 (2008).
24. K. Zhang and J. Kang, "Graphics processing unit accelerated non-uniform fast Fourier transform for ultrahigh-speed, real-time, Fourier-domain OCT," *Opt. Express* **18**, 23472–23487 (2010).